Engineering of co-ordination polymers of *trans*-4,4′-azobis(pyridine) and *trans*-1,2-bis(pyridin-4-yl)ethene: a range of interpenetrated network motifs

Matthew A. Withersby,[a] Alexander J. Blake,[a] Neil R. Champness,[a] Paul A. Cooke,[a] Peter Hubberstey,*[a] Annabel L. Realf,[a] Simon J. Teat[b] and Martin Schröder *[a]

[a] *School of Chemistry, The University of Nottingham, Nottingham, UK NG7 2RD.*
   E-mail: m.schroder@nottingham.ac.uk, peter.hubberstey@nottingham.ac.uk
[b] *CLRC Daresbury Laboratory, Daresbury, Warrington, UK WA4 4AD*

Crystallisation experiments involving cobalt(II), copper(I), copper(II) or cadmium(II) and *trans*-4,4′-azobis(pyridine) (4,4′-azpy) or *trans*-1,2-bis(pyridin-4-yl)ethene (bpe) yield $M_2(NO_3)_4(L)_3(CH_2Cl_2)(H_2O)_x$ (M = Co, L = 4,4′-azpy, x = 0 **1**; M = Cd, L = 4,4′-azpy, x = 2 **2**; M = Co, L = bpe, x = 0 **6**), $Cu(BF_4)(L)_2$ (L = 4,4′-azpy **3**; L = bpe **10**), $Cu(BF_4)_2(L)_2(H_2O)_2$ (L = 4,4′-azpy **4**; L = bpe **9**) and $Cd(NO_3)_2(bpe)$ **8**. Crystals suitable for X-ray diffraction analysis were obtained for the 4,4′-azpy complexes **1–3** and $Cu(SiF_6)(4,4′-azpy)_2(H_2O)_3$ **5**, prepared during recrystallisation of **4**, but not for any of the complexes of bpe. The molecular architectures of the 4,4′-azpy co-ordination polymer networks are metal centre dependent, the preferred co-ordination geometries of $Co(NO_3)_2$/$Cd(NO_3)_2$ (T-shaped connecting unit), Cu(I) (tetrahedral connecting unit) and Jahn–Teller distorted Cu(II) (square planar connecting unit) dictating the formation of herringbone, adamantoid and square grid constructions for $\{[M_2(NO_3)_4(\mu\text{-}4,4′\text{-azpy})_3]\cdot CH_2Cl_2\cdot xH_2O\}_\infty$ (M = Co, x = 0 **1**; M = Cd, x = 2 **2**), $\{[Cu(\mu\text{-}4,4′\text{-azpy})_2][BF_4]\}_\infty$ **3** and $\{[\{Cu(H_2O)_2\}(\mu\text{-}4,4′\text{-azpy})_2][SiF_6]\cdot H_2O\}_\infty$ **5**, respectively. All three networks display interpenetration; three-fold parallel interpenetration of novel herringbone sheets in **1** and **2**, five-fold interpenetration of adamantoid networks in **3**, and inclined perpendicular interpenetration of rhombically distorted sheets in **5**. Despite the interpenetration, cavities are present in all three of the architectures and these are filled by anions and/or guest solvent molecules.

The rational design of co-ordination polymer networks is a rapidly developing area.[1–3] Their architectures, which include one-dimensional chains[4–7] and ladders,[7–11] two-dimensional grids,[8,10–20] and three-dimensional diamondoid[21–30] and 'helical staircase'[5] networks, have been shown to be dependent upon metal ion,[1–3] ligand functionality,[1–3,21–23] anion[5,6] and reaction solvent.[7] The geometries of the metal ion and ligand connecting units control the dimensionality of the network,[1–3] the functionality of the ligand determines the intra-network spacing,[21–23] weakly co-ordinating anions influence the symmetry of the network,[5] and protic co-ordinating solvents of crystallisation provide the opportunity for supramolecular hydrogen-bonding interactions.[7,13,17–20]

Bridging ligands, commonly 4,4′-bipyridyl systems, can be rigid (so-called molecular rods) or flexible, and in developing molecular rods, we have concentrated, thus far, on varying their length and bulk. For example, by increasing the length of the linker from 7.1 Å [for 4,4′-bipyridine (4,4′-bipy; Scheme 1)] to 9.4 Å [for *trans*-1,2-bis(pyridin-4-yl)ethene (bpe; Scheme 1)] in the copper(I) co-ordination polymers $\{[Cu(\mu\text{-}L)_2]^+\}_\infty$ (L = 4,4′-bipy or bpe) the degree of interpenetration of the three-dimensional adamantoid architecture increases from four-fold[21] to five-fold.[22] We have also considered steric effects. Thus, by increasing the bulk of the bridging ligand from 4,4-bipy to 2,7-diazapyrene (2,7-diaz; Scheme 1) the degree of interpenetration of the three-dimensional adamantoid architecture of $\{[Cu(\mu\text{-}L)_2]^+\}_\infty$ (L = 4,4′-bipy or 2,7-diaz) decreases from four-fold[21] to three-fold.[23]

We now turn our attention to an investigation of the structural ramifications arising from chemical modification of the central section of the bridging ligand. The chosen bridges, *trans*-4,4′-azobis(pyridine) (4,4′-azpy; Scheme 1) and *trans*-1,2-bis(pyridin-4-yl)ethene (bpe; Scheme 1) have –N=N– and –CH=CH– moieties, respectively, linking two pyridyl donors.
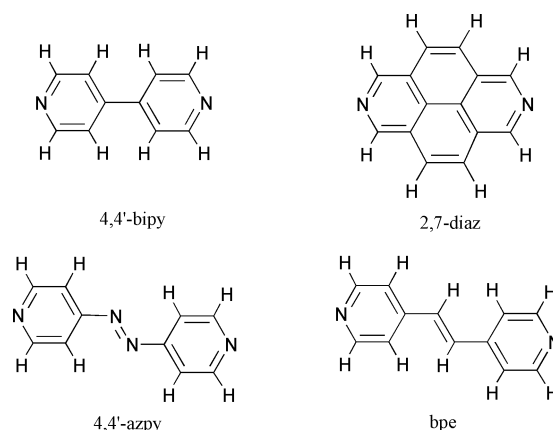
Scheme 1 Bridging ligands.

The principal difference between the bridging ligands lies in the ease of generation of planar conformations. Weak hydrogen-bonding contacts between the C–H moiety at the 3-position of the pyridine ring and the diazo linking units of 4,4′-azpy could promote planarity, while the corresponding C–H moieties in bpe could sterically clash with the adjacent C–H groups of the ethene link to disfavour planarity. We now report herein results of a synthetic and structural study of the co-ordination polymers formed by Co[II], Cu[I], Cu[II] and Cd[II] when linked by 4,4′-azpy or bpe. Although crystalline products were obtained throughout, only the 4,4′-azpy bridged products were suitable for single crystal X-ray diffraction analysis. Consequently unambiguous structural data could only be obtained for $\{[M_2(NO_3)_4(4,4′\text{-}\mu\text{-azpy})_3]\cdot CH_2Cl_2\cdot xH_2O\}_\infty$ (M = Co, x = 0 **1**; M = Cd, x = 2 **2**) which exhibit parallel interpenetration of herringbone sheets, for $\{[Cu(\mu\text{-}4,4′\text{-azpy})_2][BF_4]\}_\infty$ **3** which

Table 1 Reaction stoichiometries and product analyses

Product	Metal salt[a]			Yield			Product analysis(calc.) (%)			Colour
	g	mol (×10⁵)	L:M	g	mol (×10⁵)	%	C	H	N	
1 $Co_2(NO_3)_4(4,4'$-azpy$)_3$-(CH_2Cl_2)	0.039	13.40	2.03	0.013	1.30	19	35.95 (37.10)	2.70 (2.60)	22.10 (22.35)	Red
2 $Cd_2(NO_3)_4(4,4'$-azpy$)_3$-$(CH_2Cl_2)(H_2O)_2$	0.042	13.62	1.99	0.016	1.42	21	32.80 (32.50)	2.35 (2.65)	20.35 (19.55)	Red
3 $Cu(BF_4)(4,4'$-azpy$)_2$	0.028	8.90	3.05	0.012	2.31	26	45.15 (46.30)	3.20 (3.10)	20.75 (21.60)	Black
4 $Cu(BF_4)_2(4,4'$-azpy$)_2(H_2O)_2$	0.220	71.15	2.07	0.205	32.02	45	36.35 (37.45)	2.50 (3.15)	17.55 (17.45)	Brown
5 $Cu(SiF_6)(4,4'$-azpy$)_2(H_2O)_3$	0.050	24.32	2.05	0.108	17.20	71	38.45 (38.25)	3.45 (3.50)	18.00 (17.85)	Brown
6 $Co_2(NO_3)_4(bpe)_3(CH_2Cl_2)$	0.040	13.71	1.98	0.020	1.85	27	44.60 (44.55)	3.60 (3.25)	14.05 (14.05)	Pink
7 $Cu(NO_3)_2(bpe)_2(CH_2Cl_2)$	0.033	13.66	1.99	0.068	10.68	79	47.60 (47.15)	3.55 (3.50)	13.60 (13.20)	Blue
8 $Cd(NO_3)_2(bpe)$	0.042	13.71	1.98	0.031	7.40	54	34.60 (34.45)	2.25 (2.40)	13.05 (13.40)	Colourless
9 $Cu(BF_4)_2(bpe)_2(H_2O)_2$	0.040	13.48	2.01	0.049	7.68	57	45.40 (45.20)	3.85 (3.80)	8.50 (8.80)	Blue

[a] Metal salts: $Co(NO_3)_2 \cdot 6H_2O$, $[Cu(NCMe)_4][BF_4]$, $Cu(BF_4)_2 \cdot xH_2O$ ($x = 4.0$ by analysis), $Cu(SiF_6)$, $Cu(NO_3)_2 \cdot 3H_2O$, $Cd(NO_3)_2 \cdot 4H_2O$. The same amount of ligand (0.05 g, 27.14×10^{-5} mol) was used in each experiment except for the preparation of $Cu(BF_4)_2(4,4'$-azpy$)_2(H_2O)_2$ (0.271 g, 147.12×10^{-5} mol) and $Cu(SiF_6)(4,4'$-azpy$)_2(H_2O)_3$ (0.092 g, 49.94×10^{-5} mol).

Table 2 IR Spectroscopic data for 4,4'-azpy- and bpe-bridged co-ordination polymers

Product	IR of ligand/cm⁻¹												IR of anion/cm⁻¹
4,4'-azpy	—	1586s	1565s	1490m	1414s	1322m	1242m	1224s	989m	837s	567s	521s	
1	3185br	1603m	—	1472m	1417m	1305w	—	1226w	1014w	845m	570w	546w	1384s
2	3455br	1600s	1570w	1452s	1418s	1330w	1292s	1227m	1013m	843m	568m	540w	1384s
3	3440br	1587m	1563w	1486m	1414m	—	1240w	1224w	—[a]	835s	567m	521w	1084s
4	3425br	1603m	1567w	1493w	1423m	1310w	—	1227w	—[a]	850m	556m	532w	1060s, br
5	3449br	1610s	1571w	1493w	1422s	—	—	1231m	1050m	868s	—[a]	—[a]	697s, br, 620m, br, 480m
bpe	—	1596s	1555w	1414m	1220w	992s	982s	823s	553s				
6	3415br	1611s	1507w	1428w	1208w	1018w	985w	831w	553m				1383s
7	3415br	1614s	1508w	—	1208w	1025w	984w	833m	553m				1384s
8	3445br	1611s	—[a]	1435m	1208w	1024m	980m	833m	549m				1493s, 1384s, 1289s
9	3420br	1613s	1508w	1431w	1208w	1031sh	981m	835m	554m				1080s, br

[a] Masked by anion vibrations.

exhibits interpenetrated adamantoid networks, and for {[Cu-$(H_2O)_2(\mu$-4,4'-azpy$)_2$][SiF$_6$]·H$_2$O}$_\infty$ **5** which exhibits interpenetrated rhombically distorted square-grids. Structural information for the bpe compounds could only be inferred by comparison with their 4,4'-azpy analogues. The structures of {[M$_2$(NO$_3$)$_4(\mu$-4,4'-azpy$)_3$]·CH$_2$Cl$_2$·xH$_2$O}$_\infty$ (M = Co, x = 0 **1**; M = Cd, x = 2 **2**) have been reported previously in the form of a preliminary communication.[31]

Results and discussion

Layering experiments using either M(NO$_3$)$_2$·xH$_2$O (M = Co or Cd) in EtOH or [Cu(MeCN)$_4$][BF$_4$] in MeCN with 4,4'-azpy in CH$_2$Cl$_2$ yielded crystals suitable for X-ray structural study. Initially characterised by chemical and spectroscopic methods (Tables 1 and 2), the crystals were subsequently shown to be {[M$_2$(NO$_3$)$_4(\mu$-4,4'-azpy$)_3$]·CH$_2$Cl$_2$·xH$_2$O}$_\infty$ (M = Co, x = 0 **1**; M = Cd, x = 2 **2**) and {[Cu(μ-4,4'-azpy$)_2$][BF$_4$]}$_\infty$ **3**, respectively. The corresponding experiment with Cu(BF$_4$)$_2$·xH$_2$O yielded a microcrystalline product for which chemical and spectroscopic analysis (Tables 1 and 2) suggested the formulation, Cu(BF$_4$)$_2$-(4,4'-azpy$)_2$(H$_2$O)$_2$ **4**. Recrystallisation by vapour phase diffusion of Et$_2$O into a solution of **4** in aqueous MeCN (1:1, v/v) gave a limited number of tiny crystals which were shown, by X-ray methods, to be {[{Cu(H$_2$O)$_2$}(μ-4,4'-azpy$)_2$][SiF$_6$]·H$_2$O}$_\infty$ **5**, a compound which was subsequently prepared by direct reaction of CuSiF$_6$ and 4,4'-azpy.

Analogous layering experiments between M(NO$_3$)$_2$·xH$_2$O (M = Co, Cu or Cd) or Cu(BF$_4$)$_2$·xH$_2$O in EtOH with bpe in CH$_2$Cl$_2$ yielded either powders or poorly crystalline products

not suitable for single crystal X-ray analysis. Chemical and spectroscopic analysis (Tables 1 and 2) suggested the formulations, Co$_2$(NO$_3$)$_4$(bpe$)_3$(CH$_2$Cl$_2$) **6**, Cu(NO$_3$)$_2$(bpe$)_2$(CH$_2$Cl$_2$) **7**, Cd(NO$_3$)$_2$(bpe) **8** and Cu(BF$_4$)$_2$(bpe$)_2$(H$_2$O)$_2$ **9**. The reaction with [Cu(MeCN)$_4$][BF$_4$] was not studied as earlier work had shown the product to be {[Cu(μ-bpe$)_2$][BF$_4$]}$_\infty$ **10**.[22] In a determined attempt to generate crystals suitable for X-ray study, the reactions were carried out using methanol or propan-2-ol instead of ethanol. Precipitates, which were shown to be identical to the products isolated from EtOH, were invariably obtained.

Molecular structures of {[M$_2$(NO$_3$)$_4(\mu$-4,4'-azpy$)_3$]·CH$_2$Cl$_2$·xH$_2$O}$_\infty$ (M = Co, x = 0 **1**; M = Cd, x = 2 **2**)

The structures of **1** and **2** have been described in detail in a preliminary communication;[31] a brief resumé follows. They are virtually identical, the only difference being the presence of lattice water in **2**. The metal co-ordination spheres adopt distorted pentagonal bipyramidal co-ordination geometries. They comprise two axial and one equatorial pyridyl donors and two equatorial bidentate nitrates. The T-shaped connecting units are linked to give a two-dimensional herringbone architecture which runs parallel to the (1 0 1) plane (Fig. 1).

The herringbone sheets can be described as (6,3) co-ordination networks, i.e. each metal centre is connected to three other metal centres by 4,4'-azpy ligands and the shortest closed circuit consists of six of these metal nodes. Two crystallographically independent bridging ligands link the six metal centres in an $f f g f f g$ sequence (Scheme 2). This arrangement contrasts with the (6,3) network in brick-wall constructions,[9] in
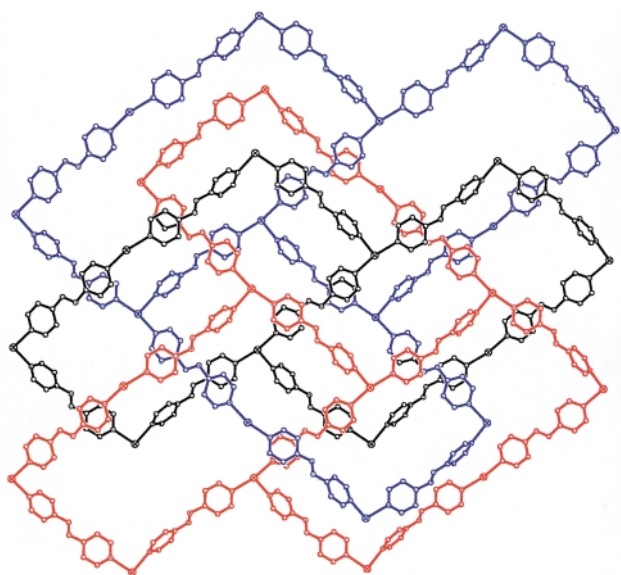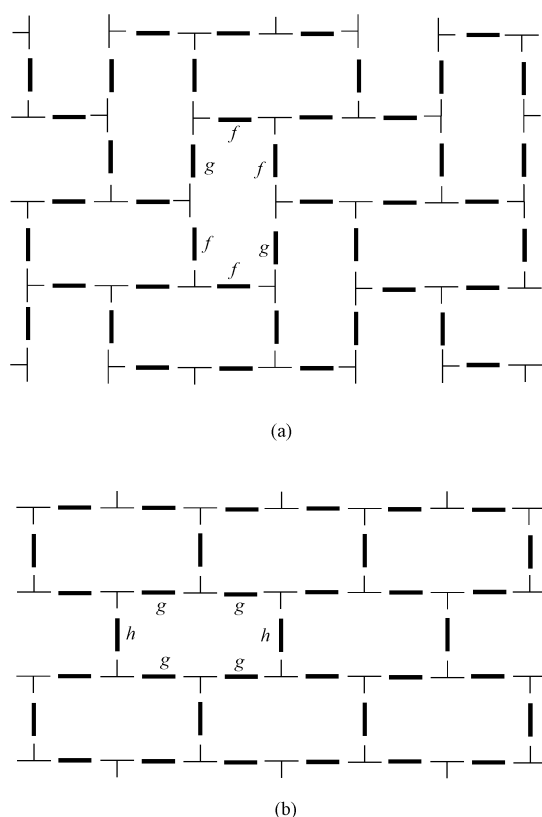
Fig. 1 View of the structure of $\{[Co_2(NO_3)_4(\mu\text{-}4,4'\text{-azpy})_3]\cdot CH_2Cl_2\}_\infty$, perpendicular to the (1 0 1) plane, showing three interpenetrated herringbone sheets (nitrate anions and solvent molecules have been omitted for clarity).

**Scheme 2** Schematic representations of (a) herringbone and (b) brickwall two-dimensional sheets.

which the bridging ligands link the six metal centres in a *g g h g g h* sequence (Scheme 2). The *f*-type ligands provide the end of one tile and a half-side of an adjacent tile; the *g*-type ligands provide half-sides for two adjacent tiles; the *h*-type ligands provide the ends for two adjacent tiles. Whereas the *g*-type bridges in **1** and **2** are centrosymmetric and planar, the two pyridyl units of the *f*-type bridges are crystallographically independent with large dihedral angles (55.5° for **1**, 64.0° for **2**). In both polymers the planar *g*-type bridges generate slightly longer metal-$\cdots$metal separations than the twisted *f*-type ones (for **1**, Co$\cdots$Co 13.357 and 13.304 Å; for **2** Cd$\cdots$Cd 13.305 and 13.150 Å).

Table 3 Dihedral angles (°) around the metal connecting units in $\{[M_2(NO_3)_4(\mu\text{-}4,4'\text{-azpy})_3]\cdot CH_2Cl_2\cdot xH_2O\}_\infty$ (M = Co, x = 0 **1**; M = Cd, x = 2 **2**)

	1	2		1	2
leg/arm1	56.6	61.5	leg/arm2	73.5	80.1
arm1/arm2	18.9	18.7	leg/nitrates	30.4	25.0

The non-planarity of the *f*-type ligands is necessary to accommodate the three pyridyl donors at the T-shaped metal centres. To minimise steric repulsion and to maximise efficient packing, the pyridyl donor which forms the leg of the T is approximately perpendicular to those which form the arms of the T. For the same reasons, it is more closely coplanar with the bidentate nitrates. Pertinent dihedral angles are quoted in Table 3.

The cationic herringbone sheets contain large rectangular cavities, which are occupied by two other, symmetry-related, herringbone sheets intertwined in a parallel fashion (Fig. 1). This three-fold interpenetration is facilitated by the undulation of the herringbone sheets which gives them a corrugated appearance. The periodicity of the undulations (**1**: 33.37 Å, **2**: 33.50 Å) is equal to three translations along the *b*-axis, the direction of propagation of the corrugation (Scheme 3). Alternatively it can be considered to correspond to an *f g f g f g* sequence of bridges in the *b* direction (Scheme 3). The sequence of bridges in the perpendicular direction (along the *ac* diagonal) is *f f f f f f* (Scheme 3).
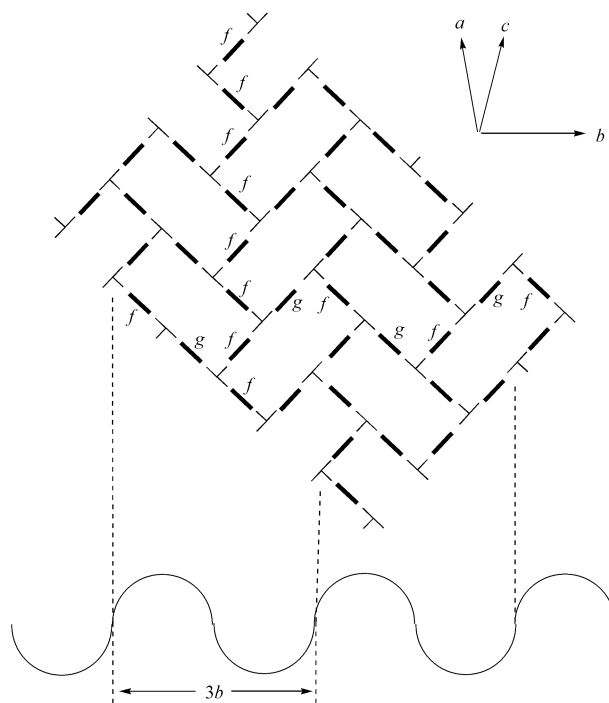
Scheme 3 Schematic diagram showing the periodicity of the undulations of the herringbone sheet.

Despite the parallel interpenetration of the herringbone sheets in **1** and **2**, cavities remain between adjacent interpenetrated layers (14.2% by volume in **1**, and 15.1% in **2**)[32] and these are filled by guest solvent molecules (CH_2Cl_2 in **1**; CH_2Cl_2 and H_2O in **2**).[32]

Molecular structure of $\{[Cu((\mu\text{-}4,4'\text{-azpy})_2][BF_4]\}_\infty$ 3

Structural features of **3** are shown in Figs. 2–4. The Cu^I centre (Fig. 2), which is located on a site with crystallographically imposed $\bar{4}$ symmetry, is co-ordinated by four [N(31)] pyridyl
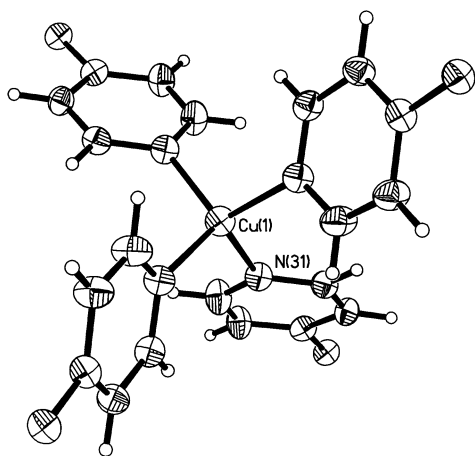
Fig. 2 Co-ordination geometry of the copper(II) centre in {[Cu(μ-4,4′-azpy)₂][BF₄]}∞ **3**.
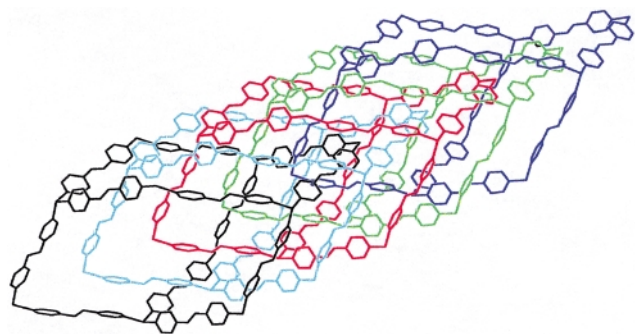
Fig. 3 View of the structure of {[Cu(μ-4,4′-azpy)₂][BF₄]}∞, showing the five-fold interpenetration of the adamantoid networks (tetrafluoroborate anions have been omitted for clarity).

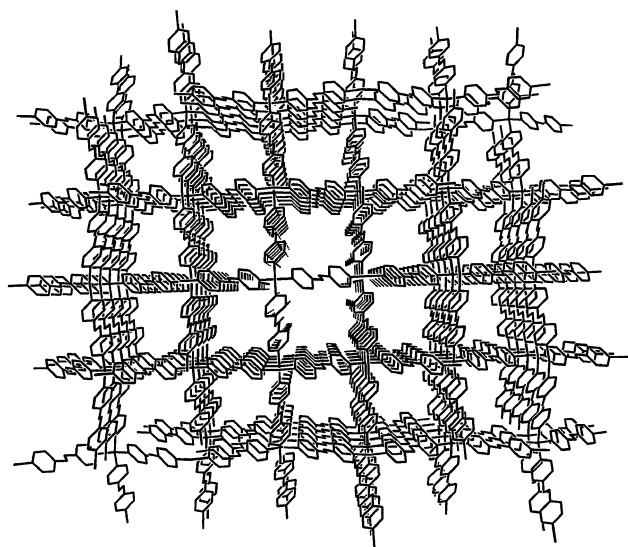**Fig. 4** View of the structure of {[Cu(μ-4,4′-azpy)₂][BF₄]}∞ showing the channels resulting from the interpenetration of the adamantoid networks (tetrafluoroborate anions have been omitted for clarity).

donors in a tetrahedral arrangement [Cu · · · N 2.034(3) Å; N–Cu–N 103.7(2), 112.44(9)°]. Each pyridyl donor forms part of a centrosymmetric, planar, 4,4′-azpy ligand, which bridges to another copper(I) centre (Cu · · · Cu 12.980 Å) to give a three-dimensional cationic adamantoid (diamondoid) (6,4) network. The large cavity present within each adamantoid cage is filled by interpenetration of four other, symmetry-related, adamantoid networks giving a total of five interpenetrating networks (Fig. 3). Despite this interpenetration, channels (22.8% by volume),[32] which are occupied by BF_4^- anion, extend throughout the structure (Fig. 4).

Table 4 Selected bond distances (Å) and angles (°) for {[Cu(H₂O)₂-(μ-4,4′-azpy)₂][SiF₆}·H₂O}∞

Cu–N(31)	2.032(2)	N(31)–Cu–N(31)^i	92.37(8)
Cu–O(1)	2.342(2)	N(31)–Cu–N(31)^{ii}	177.41(8)
		N(31)–Cu–N(31)^{iii}	87.68(8)
		N(31)–Cu–O(1)	91.29(4)

i $x - 1/2$, $y + 1/2$, $-z + 1/2$; ii $-x + 1$, $-y + 1$, $-z + 1/2$; iii $-x + 3/2$, $-y + 1/2$, z.
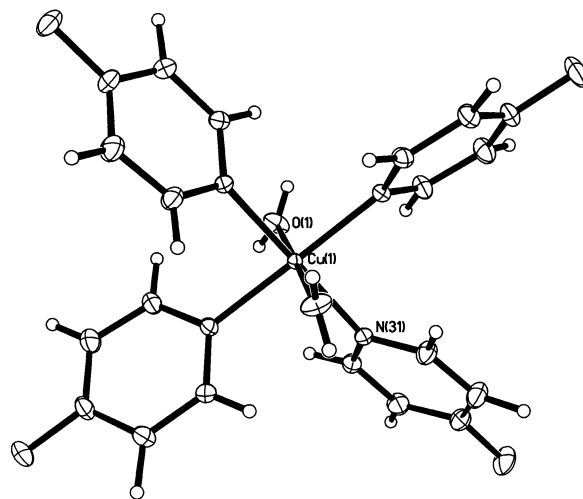
Fig. 5 Co-ordination geometry of the copper(II) centre in {[{Cu-(H₂O)₂}(μ-4,4′-azpy)₂][SiF₆]·H₂O}∞ **5**.
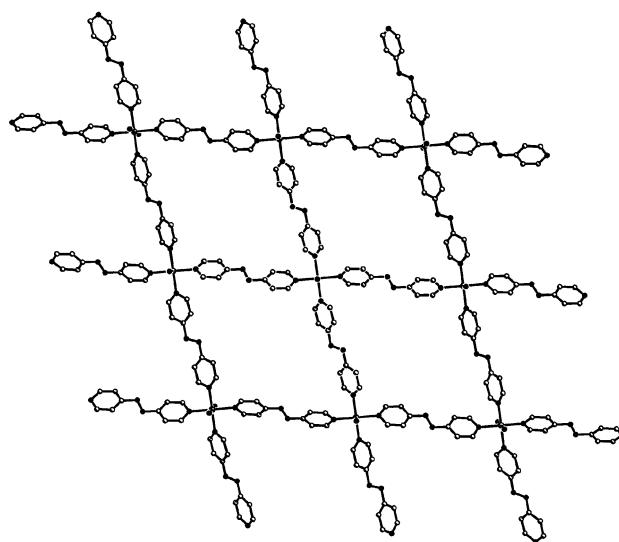
Fig. 6 The rhombically distorted square grid network formed in the structure of {[{Cu(H₂O)₂}(μ-4,4′-azpy)₂][SiF₆]·H₂O}∞ (hexafluorosilicate anions and lattice water molecules have been omitted for clarity).

Molecular structure of {[Cu(H₂O)₂(μ-4,4′-azpy)₂][SiF₆]·H₂O}∞ 5

Structural features of **5** are shown in Figs. 5–7 and selected interatomic distances and angles are quoted in Table 4. The copper(II) centre is located at the intersection of three, two-fold symmetry axes with four symmetry-related equatorial [N(31)] pyridyl donors and two symmetry related axial [O(1)] water molecules in a distorted octahedral co-ordination geometry (Fig. 5). The copper(II) centres act as square-planar connecting units which are linked by centrosymmetric planar 4,4′-azpy ligands (Cu · · · Cu 12.982 Å) to form a rhombically distorted square-grid (4,4) network (Fig. 6). The cavities in the grid are filled by perpendicular interpenetration of further sheets which lie along the square diagonal. The interpenetration leads to the formation of narrow channels (17.0% by volume)[32] which lie

Table 5 Unit cell dimensions for $\{[M_2(NO_3)_4(\mu-L)_3]\cdot wCH_2Cl_2\cdot xH_2O\cdot yMeOH\}_{\infty}$ co-ordination polymers

	Metal	Bridge	w	x	y	$a/\text{Å}$	$b/\text{Å}$	$c/\text{Å}$	$\beta/^\circ$	$V/\text{Å}^3$	Ref.
1	Co	4,4′-azpy	1	0	0	20.802(9)	11.124(4)	20.806(9)	119.27(4)	4200(3)	This work
2	Cd	4,4′-azpy	1	2	0	21.197(5)	11.166(12)	21.389(4)	122.24(2)	4282(5)	This work
12	Cd	4,4′-azpy	0	0	0	21.044(3)	10.811(2)	20.849(3)	117.31(1)	4215(1)	10
13	Co	bpethy	0	0	2	20.655(5)	11.348(2)	22.183(6)	122.76(2)	4373(2)	11
14	Cd	bpethy	1	0	0	20.682(9)	11.244(3)	20.821(9)	112.80(4)	4464(3)	10
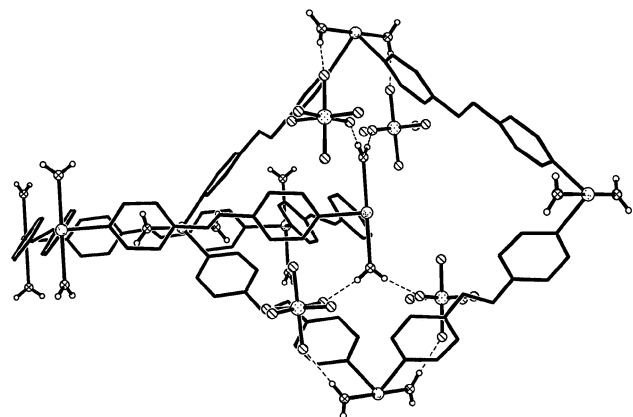
Fig. 7 View of the structure of $\{[\{Cu(H_2O)_2\}(\mu-4,4'-azpy)_2][SiF_6]\cdot H_2O]\}_{\infty}$, showing the hydrogen-bonding interactions between co-ordinated water molecules and hexafluorosilicate anions which control the perpendicular arrangement of the interpenetrated rhombically distorted square grids.

along the c direction and which are filled by SiF_6^{2-} anions and solvent water guest molecules.

Molecular structures of the bpe complexes

The products of the reactions between $M(NO_3)_2\cdot xH_2O$ (M = Co, Cu or Cd) or $Cu(BF_4)_2\cdot xH_2O$ in MeOH, EtOH or Pr^iOH with bpe in CH_2Cl_2 were independent of solvent. Chemical and spectroscopic analysis (Tables 1 and 2) suggested the formulations, $Co_2(NO_3)_4(bpe)_3(CH_2Cl_2)$ **6**, $Cu(NO_3)_2(bpe)_2$-(CH_2Cl_2) **7**, $Cd(NO_3)_2(bpe)$ **8** and $Cu(BF_4)_2(bpe)_2(H_2O)_2$ **9**.

The stoichiometry of the $Co(NO_3)_2$–bpe complex **6** is identical to that of the $Co(NO_3)_2$–4,4′-azpy complex **1**. Similarly, the stoichiometries of the $Cu(BF_4)_2$–bpe complex **9** and of the $Cu(BF_4)_2$–4,4′-azpy complex **4** are identical. The same applies for the copper(I) complexes $\{[Cu(\mu-bpe)_2][BF_4]\}_{\infty}$ **10**, which had been studied earlier,[22] and $\{[Cu(\mu-azpy)_2][BF_4]\}_{\infty}$ **3**. However, the stoichiometry of the $Cd(NO_3)_2$–bpe complex **8** (M : L = 1 : 1) differs from that of the $Cd(NO_3)_2$–4,4′-azpy complex **2** (M : L = 2 : 3) and that of a previously reported $Cd(NO_3)_2$–bpe complex, $\{[Cd_2(NO_3)_4(\mu-bpe)_3]\}$ **11**, crystallised in layering experiments involving $Cd(NO_3)_2\cdot4H_2O$ in water and bpe in ethanol.[33] Although unusual, the formation of complexes with differing stoichiometries is not unprecedented, products often varying with crystallisation solvent.[7]

X-ray diffraction studies, both single crystal and powder, showed all the bpe containing products of the present work to be amorphous. In the absence of definitive data, further conclusions concerning their structures cannot be drawn since similar stoichiometries are insufficient for inference of structural information. Thus although the 1 : 1 $Cu[BF_4]$–bpe and –4,4′-azpy complexes, **10**[22] and **3**, have similar structures, the 2 : 3 $Cd[NO_3]_2$–bpe and –4,4′-azpy complexes **11**[33] and **2** have different structures.

Discussion of architectures: herringbone sheets

Although the T-shaped geometry of the bridging ligands at the cobalt(II) and cadmium(II) centres is not unusual, the two-dimensional herringbone architecture (Fig. 1) was unknown

prior to our preliminary publication,[3] which coincided with two other publications on similar complexes, $\{[Cd_2(NO_3)_4(\mu-4,4'-azpy)_3]\}_{\infty}$ **12**,[10] $\{[Co_2(NO_3)_4(\mu-bpethy)_3]\cdot2MeOH\}_{\infty}$ [bpethy = 1,2-bis(pyridin-4-yl)ethyne] **13**[11] and $\{[Cd_2(NO_3)_4(\mu-bpethy)_3]\cdot CH_2Cl_2\}_{\infty}$ **14**.[10] Previously T-shaped connecting units had given one-dimensional ladder,[7–9] two-dimensional brick-wall,[9] and three-dimensional frame[34] (also known as 'Lincoln Logs'), 'tongue and groove'[35] and modified brick-wall[36] structures. The herringbone and brick-wall architectures can be considered to be structural isomers. They are both derived from a honeycomb motif, the (6,3) co-ordination network with three-fold symmetry, by modification of the angles at the metal centre from $3 \times 120^\circ$ to $(2 \times 90^\circ) + (1 \times 180^\circ)$. The only difference lies in the sequence in which the resulting T-shaped connecting units are oriented: T ⊥ T ⊥ (brick-wall) and ⊢ T ⊥ ⊣ (herringbone). As yet there are too few structures available for us to be able to identify those factors which determine the choice of architecture.

Co-ordination polymers **1**, **2**, **12**, **13** and **14** crystallise in the same space group ($C2/c$) with similar unit cell dimensions (Table 5) and structures. The only difference between polymers **2** and **12** is the inclusion of solvent molecules in the structure of **2**. The two polymers were crystallised from slightly different reactant systems (**2**: molar ratio L : M = 2 : 1; solvents CH_2Cl_2–EtOH; **12**: molar ratio L : M = 2 : 1; solvents CH_2Cl_2–Me_2CO). The observation that inclusion/exclusion of solvent does not affect the choice of network architecture for these polymers infers an inherent stability for this structural motif.

Parallel three-fold interpenetrated (6,3) co-ordination polymers are not restricted to those based on a herringbone motif. A single example, $\{[Cd_2(NO_3)_4(\mu-L)_3]\}_{\infty}$ [L = 1,4-bis(pyridin-4-yl)methyl-2,3,5,6-tetrafluorobenzene], of an analogous construction based on the interleaving of a brick-wall motif has been reported.[8]

Adamantoid networks

The adamantoid based motif adopted by **3** (Fig. 3) is a (6,4) co-ordination network. It can be referred to as a super-diamondoid network as it structurally related to diamond, each carbon in diamond being replaced by a copper(I) centre and each C–C bond being replaced by a 4,4′-azpy linker. Such networks have been observed for a small number of cationic co-ordination polymers $\{[CuL_2]^+\}_{\infty}$ with nitrile and pyridyl donor bridging ligands (Table 6). Significant points which arise from a correlation of the degree of interpenetration in these structures with the metal–metal separation (Table 6) include (i) increased length of spacer generally leads to increased interpenetration; (ii) nitrile bridges exhibit greater degrees of interpenetration than pyridyl bridges (e.g., N,N'-dicyanoquinodiimine (Cu⋯Cu 12.76 Å) and 4,4′-azopyridine (Cu⋯Cu 12.98 Å) and generate systems with similar metal–metal separations but with seven and five interpenetrated nets, respectively); (iii) increasing the bulk of the bridging ligand reduces the degree of interpenetration [e.g., substituting terephthalonitrile (1,4-dicyanobenzene) in the 2 and 3 positions with methyl groups reduces the number of interpenetrated nets from five to three despite an identical copper-copper separation (11.91 Å) and changing the linker from 4,4′-bipyridine (Cu⋯Cu 11.16 Å) to 2,7-diazapyrene (Cu⋯Cu 10.90 Å) reduces the number of interpenetrated nets from four to three].

Table 6 {[CuL$_2$]$^+$}$_\infty$ cationic co-ordination polymers with interpenetrated adamantoid (6,4) networks

Bridging ligand (L)	Number of interpenetrated nets	Cu···Cu/Å	Ref.
2,3-Dimethylterephthalonitrile	3	11.91	27
Terephthalonitrile	5	11.91	28
1,4-Dicyanobutane	6	12.9	29
2,5-Dimethyl-*N,N'*-dicyanoquinodiimine	7	12.76	30
4-Cyanopyridine	2	9.34	1
2,5-Dimethylpyrazine	1	6.99	26
2,7-Diazapyrene	3	10.90	23
4,4'-Bipyridine	4	11.16	21
trans-1,2-Bis(pyridin-4-yl)ethene	5	13.55	23
4,4'-Azopyridine	5	12.98	This work
1,4-Bis(pyridin-4-yl)butadiyne	6	15.95	1

As for the interpenetrated herringbone structure, the integrity of the adamantoid structure is such that neither changing bridging ligand type nor inclusion/exclusion of guest solvent molecules has any effect on the choice of network architecture. Furthermore, we believe that it is now possible to control the degree of interpenetration of (6,4) nets since it is a well established function of spacer ligand length, donor type and bulk.
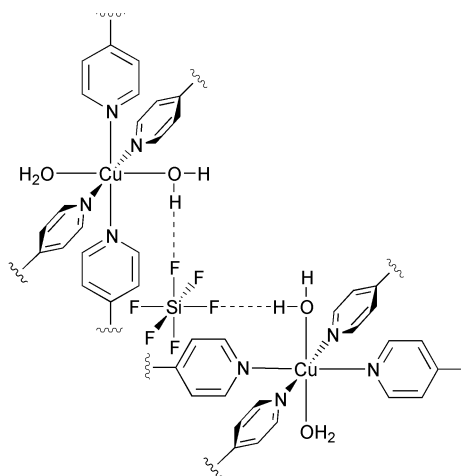
Square-grid sheets

The two-dimensional (4,4) square-grid network formed by **5** (Fig. 6), in which metal centres are linked by co-ordinatively bonded bridging bipyridyls, is well established in Co(II),[13] Ni(II),[12] Zn(II)[15,16] and Cd(II)[14] co-ordination polymer chemistry. The metal centres adopt tetragonally distorted octahedral geometries with four equatorial pyridyl donors and either two axial anions or two axial water molecules. A similar two-dimensional (4,4) rectangular network, in which metal centres are linked in one direction by co-ordinatively bonded bridging bipyridyls and in the other by bridging bipyridyls hydrogen-bonded to co-ordinated water or methanol (M–O–H···N$^\cap$N···H–O—M), has been described for Mn(II),[20] Fe(II),[18,19] Co(II),[13] Cu(II)[17] and Zn(II)[18] co-ordination polymers. The metal centres are effectively distorted octahedral with two equatorial pyridyl donors and two equatorial water molecules with two axial anions.

The rectangular networks ({[Mn(MeOH)$_2$(NCS)$_2$(μ-bpe)]·bpe}$_\infty$,[20] {[Fe(MeOH)$_2$(NCS)$_2$(μ-4,4'-azpy)]·4,4'-azpy}$_\infty$,[19] {[Fe(H$_2$O)$_2$(NCS)$_2$(μ-4,4'-bipy)]·4,4'-bipy}$_\infty$,[19] {[Fe(H$_2$O)$_3$(OClO$_3$)-(μ-4,4'-bipy)][ClO$_4$]·1.5(4,4'-bipy)·H$_2$O}$_\infty$,[18] {[Co(H$_2$O)$_2$-(NCS)$_2$(μ-4,4'-bipy)]·4,4'-bipy}$_\infty$,[13] {[Cu(H$_2$O)$_2$(BF$_4$)$_2$(μ-4,4'-bipy)]·4,4'-bipy}$_\infty$,[17] {[Zn(H$_2$O)$_4$(μ-4,4'-bipy)][NO$_3$]$_2$·4,4'-bipy}$_\infty$,[18] {[Zn(H$_2$O)$_4$(μ-4,4'-bipy)][NO$_3$]$_2$·2(4,4'-bipy)·3H$_2$O}$_\infty$,[18] {[Zn(H$_2$O)$_4$(μ-4,4'-bipy)][O$_3$SCF$_3$]$_2$·2(4,4'-bipy)}$_\infty$[18]) form similar structures based on layered non-interpenetrated sheets.

The square networks adopt a range of topologies. Layered non-interpenetrated sheets are formed in {[Co(NCS)$_2$(μ-4,4'-bipy)$_2$]·Et$_2$O}$_\infty$,[13] {[{Cd(NO$_3$)$_2$}(μ-4,4'-bipy)$_2$]}$_\infty$[14] and {[Zn$_2$-(μ-SiF$_6$)$_2$(μ-4,4'-bipy)$_2$]·xDMF}$_\infty$.[16] The only difference in these structures lies in the anion role; hexafluorosilicate bridges sheets of {[Zn(μ-4,4'-bipy)$_2$]$^{2+}$}$_\infty$, whereas thiocyanate and nitrate locate in the cavities of adjacent sheets of {[M(μ-4,4'-bipy)$_2$]$^{2+}$}$_\infty$ (M = Co or Cd). Layered networks are also found in the Ni(II) co-ordination polymer {[Ni(ONO$_2$)$_2$(μ-4,4'-azpy)$_2$]-{Ni$_2$(NO$_3$)$_4$(μ-4,4'-azpy)$_3$}·4CH$_2$Cl$_2$}$_\infty$.[12] In this case, however, parallel {[Ni(μ-4,4'-azpy)$_2$]$^{2+}$}$_\infty$ square networks perpendicularly interpenetrate {[Ni$_2$(NO$_3$)$_4$(μ-4,4'-azpy)$_3$]}$_\infty$ brick-wall constructions.

Complex **5** and its Zn(II) analogues, {[Zn(H$_2$O)$_2$(μ-4,4'-bipy)$_2$][SiF$_6$]}$_\infty$[15] and {[Zn(H$_2$O)$_2$(μ-4,4'-azpy)][SiF$_6$]·H$_2$O}$_\infty$,[12] all form perpendicularly-interpenetrated structures with inclination angles of 45° (Scheme 4). We believe the presence of both co-ordinated water and lattice SiF$_6$$^{2-}$ is essential for the gener-

Scheme 4 Schematic representation of the H$_2$O···SiF$_6$$^{2-}$···H$_2$O hydrogen bonding contacts linking the perpendicularly interpenetrated rectangular grids in {[Cu(H$_2$O)$_2$(μ-4,4'-azpy)$_2$][SiF$_6$]·H$_2$O} **5**.

ation of these perpendicularly-interpenetrated structures. They are involved in a series of hydrogen-bonded contacts [O(1)–H(11)···F(5); O···F 2.683 Å, O–H 0.83 Å, H···F 1.86 Å, O–H···F 170.6°; O(1)–H(12)···F(6); O···F 2.728 Å, O–H 0.85 Å, H···F 1.88 Å, O–H···F 180.0°; Fig. 7] which generate an intersheet angle of *ca.* 90°. An analogous interaction is responsible for the interpenetration of the nearly perpendicular (dihedral angle 74°) square networks in the structure of {[Cu-(μ-bpe)$_2$][Cu(H$_2$O)$_2$(SO$_4$)$_2$(μ-bpe)]·2H$_2$O}$_\infty$.[37] In this complex, the {[Cu(μ-bpe)$_2$]$^{2+}$}$_\infty$ square networks are linked through {[Cu(H$_2$O)$_2$(SO$_4$)$_2$(μ-bpe)]$^{2-}$}$_\infty$ chains by bridging SO$_4$$^{2-}$ anions.

Conclusion

The molecular architectures of co-ordination polymers of 4,4'-azpy are metal centre dependent, the preferred co-ordination geometries of Co(NO$_3$)$_2$/Cd(NO$_3$)$_2$ (T-shaped connecting unit), Cu(I) (tetrahedral connecting unit) and Jahn–Teller distorted Cu(II) (square-planar connecting unit) dictating the formation of herringbone, adamantoid and square-grid constructions. All three networks display interpenetration; three-fold parallel interpenetration of novel herringbone sheets in **1** and **2**, five-fold interpenetration of adamantoid networks in **3** and inclined perpendicular interpenetration of rhombically distorted square-grid sheets in **5**. Despite the interpenetration, cavities are present in all three of the architectures reported here and these are filled by anions and/or guest solvent molecules.

Owing to the paucity of structural data, it has not been possible to come to any firm conclusions regarding the influence of the –N=N– and –CH=CH– moieties linking the two pyridyl donors in 4,4'-azpy and bpe. Planar configurations predominate for both ligands, being found for 4,4'-azpy in **1**, **2**, **3** and **5**

and for bpe in **9** and **10**, although the only examples of non-planar bridges are observed for 4,4′-azpy in **1** and **2**.

Although we have been able to show that $Co(NO_3)_2$, $Cu(BF_4)$ and $Cu(BF_4)_2$ form compounds with 4,4′-azpy and bpe of identical stoichiometry, we have only been able to confirm analogous structures for the Cu(I) polymers, $\{[Cu(\mu\text{-L})_2][BF_4]\}_\infty$ (L = azpy **3**, bpe **10**). The absence of structural data for the $Co(NO_3)_2$–bpe, $Cu(BF_4)_2$–bpe and $Cu(BF_4)_2$–4,4′-azpy compounds prevents further comparison. The polymer combinations $Cd(NO_3)_2$–4,4′-azpy and $Cd(NO_3)_2$–bpe, despite identical M:L ratios (2:3), have totally different structures.

Of the three architectures—adamantoid, herringbone and square-grid networks—adamantoid networks are the least sensitive to the more subtle structure determining factors. Tetrahedral metal ion centres form adamantoid networks regardless of bridging ligand and crystallisation solvent. For example, adamantoid networks are formed in $\{[Cu(\mu\text{-L})_2]$-$[BF_4]\}_\infty$ (L = 4,4-azpy, bpe or 4,4′-bipy). The creation of herringbone sheets from T-shaped metal ion centres is not sensitive to crystallisation solvent but is dependent on choice of bridging ligand. Thus, $\{[M_2(NO_3)_4(\mu\text{-L})_3]\cdot x H_2O\cdot w CH_2Cl_2\cdot y MeOH\}_\infty$ (M = Co or Cd) exist as herringbone sheets when L = 4,4′-azpy or bpethy but as infinite non-interpenetrating zigzag molecular chains when L = bpe. Square-grid sheets are the least robust, their formation from square-planar metal ion centres being dependent on both bridge and solvent. Thus, water is an essential component of the hydrogen-bonding network required to create the perpendicularly-interpenetrating square-grid structures of $\{[M(H_2O)_2(\mu\text{-L})_2][SiF_6]\cdot x H_2O\}_\infty$ (M = Cu, L = 4,4′-azpy; M = Zn, L = 4,4′-azpy or 4,4′-bipy).

Experimental

Synthesis, general procedures

The Cu(I) starting material, $[Cu(NCMe)_4][BF_4]$, was prepared by treatment of hydrated copper(II) tetrafluoroborate with copper powder in MeCN.[38] The bridging ligand, 4,4′-azpy, was obtained by oxidation of 4-aminopyridine with sodium chlorate(I).[39] All other chemicals (Aldrich Chemical Company Ltd.) were reagent grade and were used as received. Elemental analyses (C, H, N) were carried out by the University of Nottingham Analytical Services. Infrared spectra in KBr discs, transmission UV-VIS spectra in KBr discs and ^{1}H NMR spectra in $CDCl_3$ were recorded using Nicolet Avator 360, Unicam UV2-100 and Bruker DPX 300 spectrometers, respectively.

Preparation of complexes

All complexes were formed by similar protocols. Full experimental details are collected in Table 1. IR spectroscopic data are summarised in Table 2.

Complexes 1, 2 and 6–9. A solution of the appropriate salt in methanol, ethanol or propan-2-ol (10 cm³) was layered on to a solution of the bridging ligand in dichloromethane (10 cm³). Crystals either formed at the interface of the solutions or by diffusion of Et_2O or toluene into the mother-liquor once diffusion was complete. Crystals suitable for X-ray diffraction study were only obtained for complexes **1** and **2**; amorphous products were formed for complexes **6–9**.

Complex 3. A solution of $[Cu(NCMe)_4][BF_4]$ in MeCN (10 cm³) was layered onto a solution of 4,4′-azpy in CH_2Cl_2 (10 cm³). After diffusion of the layers was complete, the mother-liquor was exposed to Et_2O vapour diffusion and red crystals suitable for X-ray diffraction were produced over a period of seven days.

Complexes 4 and 5. Dropwise addition of a hot aqueous solution (50 cm³) of hydrated copper(II) tetrafluoroborate to a

Table 7 Crystallographic summary

	3	**5**
Empirical formula	$C_{20}H_{16}BCuF_4N_8$	$C_{20}H_{22}CuF_6N_8O_3Si$
M	518.76	628.09
Crystal system	Tetragonal	Tetragonal
Space group	$I4_1/a$	$P4/ncc$
$a, b/\text{Å}$	17.327(3)	10.767(2)
$c/\text{Å}$	7.729(2)	21.030(3)
$U/\text{Å}^3$	2320.4(7)	2438.0(7)
Z	4	4
μ/mm^{-1}	0.998	1.033
$D_c/\text{Mg m}^{-3}$	1.485	1.711
Reflections collected	3219	6849
Unique reflections (R_{int})	1019 (0.0586)	1650 (0.0371)
Observed reflections $[I > 2\sigma(I)]$	856	1292
R	0.0453	0.0350
R_w	0.1260	0.0937

boiling solution of 4,4′-azpy in acetonitrile (50 cm³) gave an orange solution which, after cooling, yielded a dark orange microcrystalline solid, which analysed for complex **4** (Table 1). A limited number of tiny dark brown crystals of complex **5**, suitable for X-ray crystallography, were produced by exposing a MeCN–water (1:1, v/v) solution (100 cm³) of the dark orange solid to Et_2O vapour diffusion for a period of 7 days. Complex **5** was subsequently prepared in bulk as a dark brown powder by dropwise addition of a hot aqueous solution (50 cm³) of copper(II) hexafluorosilicate to a boiling solution of 4,4′-azpy in acetonitrile (50 cm³).

Crystallography

Details of the data collections and structure solutions for **3** and **5** are given in Table 7. Diffraction data for **3** were collected on a Stoë Stadi-4 diffractometer equipped with an Oxford Cryosystems open flow cryostat[40] operating at 150 K using ω–θ scans and graphite monochromated Mo-Kα radiation. Absorption corrections were applied using ψ-scans. Those for **5** were collected at 150 K using a Bruker SMART CCD area detector diffractometer at Station 9.8 of the SRS at Daresbury Laboratory. Both structures were solved by direct methods (SHELXS 97[41]) and refined against F^2 (SHELXL 97[42]). All non hydrogen atoms were refined with anisotropic displacement parameters. For **3**, all hydrogens were placed geometrically and allowed to ride with their parent atoms. For **5**, all hydrogens on the bridging ligand and co-ordinated water molecule were found and refined isotropically. The lattice water molecule in **5** is located on a four-fold axis. One of its hydrogen atoms was found on the four-fold axis and was refined isotropically; the other, which must be located in a general position with occupancy 0.25, could not be found.

CCDC reference number 186/2141.

See http://www.rsc.org/suppdata/dt/b0/b006543i/ for crystallographic files in .cif format.

References

1 S. R. Batten and R. Robson, *Angew. Chem.*, *Int. Ed.*, 1998, **37**, 1460; P. J. Hagrman, D. Hagrman and J. Zubieta, *Angew. Chem.*, *Int. Ed.*, 1999, **38**, 2638.
2 N. R. Champness and M. Schröder, *Curr. Opin. Solid State Mater. Sci.*, 1998, **3**, 419.

3 A. J. Blake, N. R. Champness, P. Hubberstey, W.-S. Li, M. Schröder and M. A. Withersby, *Coord. Chem. Rev.*, 1999, **183**, 117.
4 A. S. Batsanov, M. J. Begley, P. Hubberstey and J. Stroud, *J. Chem. Soc.*, *Dalton Trans.*, 1996, 1947.
5 M. A. Withersby, A. J. Blake, N. R. Champness, P. Hubberstey, W.-S. Li and M. Schröder, *Angew. Chem.*, *Int. Ed. Engl.*, 1997, **36**, 2327.
6 M. Kondo, M. Shimamura, S.-I. Noro, T. Yoshitomi, S. Minakoshi and S. Kitagawa, *Chem. Lett.*, 1999, 285.
7 M. A. Withersby, A. J. Blake, N. R. Champness, P. A. Cooke, P. Hubberstey, W.-S. Li and M. Schröder, *Inorg. Chem.*, 1999, **38**, 2259.
8 M. Fujita, Y. J. Kwon, O. Sasaki, K. Yamaguchi and K. Ogura, *J. Am. Chem. Soc.*, 1995, **117**, 7287; M. Fujita, Y. J. Kwon, O. Sasaki, K. Yamaguchi and K. Ogura, *New. J. Chem.*, 1998, **22**, 189.
9 P. Losier and M. J. Zaworotko, *Angew. Chem.*, *Int. Ed. Engl.*, 1996, **35**, 2779.
10 L. Carlucci, G. Ciani and D. Proserpio, *J. Chem. Soc.*, *Dalton Trans.*, 1999, 1799.
11 Y.-B. Dong, R. C. Layland, N. G. Pschirer, D. M. Smith, U. H. F. Bunz and H. C. zur Loye, *Chem. Mater.*, 1999, **11**, 1413.
12 L. Carlucci, G. Ciani and D. Proserpio, *New J. Chem.*, 1998, **22**, 1319.
13 J. Lu, T. Paliwala, S. C. Lim, C. Yu, T. Niu and A. J. Jacobson, *Inorg. Chem.*, 1997, **36**, 923.
14 M. Fujita, Y. J. Kwon, S. Washizu and K. Ogura, *J. Am. Chem. Soc.*, 1994, **116**, 1151.
15 R. W. Gable, B. F. Hoskins and R. Robson, *J. Chem. Soc.*, *Chem. Commun.*, 1990, 1677.
16 S. Subramanian and M. J. Zaworotko, *Angew. Chem.*, *Int. Ed. Engl.*, 1995, **34**, 2127.
17 A. J. Blake, S. J. Hill, P. Hubberstey and W.-S. Li, *J. Chem. Soc.*, *Dalton Trans.*, 1997, 913.
18 L. Carlucci, G. Ciani, D. M. Proserpio and A. Sironi, *J. Chem. Soc.*, *Dalton Trans.*, 1997, 1801.
19 S.-I. Noro, M. Kondo, T. Ishii, S. Kitagawa and H. Matsuzaka, *J. Chem. Soc.*, *Dalton Trans.*, 1999, 1569.
20 G. De Munno, D. Armentano, T. Poerio, M. Julve and J. A. Real, *J. Chem. Soc.*, *Dalton Trans.*, 1999, 1813.
21 L. R. MacGillivary, S. Subramanian and M. J. Zaworotko, *J. Chem. Soc.*, *Chem. Commun.*, 1994, 1325.
22 A. J. Blake, N. R. Champness, S. S. M. Chung, W.-S. Li and M. Schröder, *Chem. Commun.*, 1997, 1005.
23 A. J. Blake, N. R. Champness, A. N. Khlobystov, D. A. Lemenovskii, W.-S. Li and M. Schröder, *Chem. Commun.*, 1997, 1339.
24 K. A. Hirsch, S. R. Wilson and J. S. Moore, *Chem. Eur. J.*, 1997, **3**, 765.
25 S. Lopez, M. Kahraman, M. Harmata and S. W. Keller, *Inorg. Chem.*, 1997, **36**, 6138.
26 T. Otieno, S. J. Rettig, R. C. Thompson and J. Trotter, *Inorg. Chem.*, 1993, **32**, 1607.
27 T. Kuroda-Sowa, M. Yamamoto, M. Munakata, M. Seto and M. Maekawa, *Chem. Lett.*, 1996, 349.
28 R. Robson, B. F. Abrahams, S. R. Batten, R. W. Gable, B. F. Hoskins and J. Liu, in *Supramolecular architecture. Synthetic control in thin films and solids*, ed. T. Bein, ACS, Washington, D.C., 1992, p. 256.
29 Y. Knoshita, I. Matsubara, T. Higuchi and Y. Saito, *Bull. Chem. Soc.*, *Jpn.*, 1959, **32**, 1221.
30 K. Sinzger, S. Hünig, M. Joff, D. Bauer, W. Bietsch, J. U. von Schütz, H. C. Wolf, R. K. Kremer, T. Metzenthin, R. Bau, S. I. Khan, A. Lindbaum, C. L. Lengauer and E. Tillmanns, *J. Am. Chem. Soc.*, 1993, **115**, 7696.
31 M. A. Withersby, A. J. Blake, N. R. Champness, P. A. Cooke, P. Hubberstey and M. Schröder, *New J. Chem.*, 1999, **23**, 573.
32 PLATON, A. L. Spek, *Acta Crystallogr.*, *Sect. A*, 1990, **46**, C34.
33 Y.-B. Dong, R. C. Layland, M. D. Smith, N. G. Pschirer, U. H. F. Bunz and H.-C. zur Loye, *Inorg. Chem.*, 1999, **38**, 3056.
34 F. Robinson and M. J. Zaworotko, *J. Chem. Soc.*, *Chem. Commun.*, 1995, 2413; O. M. Yaghi and H. Li, *J. Am. Chem. Soc.*, 1996, **118**, 295.
35 M. Kondo, T. Yoshimitsu, K. Seki, H. Matsuzaka and S. Kitagawa, *Angew. Chem.*, *Int. Ed. Engl.*, 1997, **36**, 1725; T. L. Hennigan, D. C. MacQuarrie, P. Losier, R. D. Rogers and M. J. Zaworotko, *Angew. Chem.*, *Int. Ed. Engl.*, 1997, **36**, 972; K. N. Power, T. L. Hennigar and M. J. Zaworotko, *New J. Chem.*, 1998, 177.
36 H. Gudbjartson, K. Biradha, K. M. Poirier and M. J. Zaworotko, *J. Am. Chem. Soc.*, 1999, **121**, 2599.
37 D. Hagrman, R. P. Hammond, R. Haushalter and J. Zubieta, *Chem. Mater.*, 1998, **10**, 2091.
38 G. J. Kubas, *Inorg. Synth.*, 1979, **19**, 90.
39 E. V. Brown and G. R. Granneman, *J. Am. Chem. Soc.*, 1975, **97**, 621.
40 J. Cosier and A. M. Glazer, *J. Appl. Crystallogr.*, 1986, **19**, 105.
41 G. M. Sheldrick, SHELXS 97, *Acta Crystallogr.*, *Sect. A*, 1990, **46**, 467.
42 G. M. Sheldrick, SHELXL 97, University of Göttingen, 1997.